Article

Not peer-reviewed version

Enhancing Mechanical Strength of Photocurable 3D Printing Resin Through Potassium Titanate Additive

Soon-ki Jeong *, Namchul Cho *, Yura Choi, Jinyoung Kim, Choongjae Lee, Geonho Lee

Posted Date: 20 November 2023

doi: 10.20944/preprints202311.1232.v1

Keywords: 3D printing; photocurable polymer; acrylate polymer; mechanical properties; potassium titanate

Article

Enhancing Mechanical Strength of Photocurable 3D Printing Resin through Potassium Titanate Additive

Yura Choi, Jinyoung Kim, Choongjae Lee, Geonho Lee, Soon-ki Jeong * and Namchul Cho *

Department of Energy Engineering, Soonchunhyang University, Asan, Republic of Korea
* Correspondence: hamin611@sch.ac.kr (S.J.), chon7@sch.ac.kr (N.C.)

Abstract: Advancements in 3D printing technologies have led to new implementations in rapid prototyping, microfluidics, tooling, dentistry, biomedical devices, drug delivery, and tissue engineering. Stereolithography techniques, which are photopolymerization-based processes, contribute to the optical, chemical, and mechanical properties of 3D printed materials using versatile polymer chemistry. This study used potassium titanate powder ($K_2Ti_8O_{17}$) as an additive to enhance the mechanical strength of photocurable resins. PEG was selected as the stabilizer to optimize the dispersion and precipitation of potassium titanate. The flexural strength, hardness, and tensile strength were compared to assess the mechanical strength of the 3D printing resin. The flexural strengths of the printed specimens were in the range of 15–39 N/mm^2. The measured surface hardness and tensile strength were 41–80 HV and 2.3–15 N/mm^2, respectively. The output resolution of the potassium titanate/acrylate resin was tested using a line-pattern structure. 3D printing resin without stabilizers produced lines with a thickness of 0.3 mm, whereas 3D printing resin containing a stabilizer produced lines with a thickness of 0.2 mm. The flexural strength and pattern thickness results suggest that the potassium titanate/acrylate resin can be utilized as a 3D printer resin, suggesting new possibilities for potassium titanate materials.

Keywords: 3D printing; photocurable polymer; acrylate polymer; mechanical properties; potassium titanate

1. Introduction

Additive manufacturing (AM), also known as three-dimensional (3D) printing, is a technology that transforms computer-aided design (CAD) models into physical objects. Using tomographic data, digital slicing of CAD, and 3D scans, AM builds objects layer-by-layer without the need for machining or molds. AM enables the fabrication of customized objects on demand, based on specific application requirements. In addition, the recent transition from prototyping to rapid manufacturing has prompted new projects for mechanical engineers and material experts [1]. The first version of stereolithography (SLA) 3D printing technology based on AM was invented by Charles Hull in 1986 [2,3]. 3D printing technology was introduced in the 1980s to fabricate customized or complex objects without the need for molds or machining [3,4]. Initially, 3D printing technology was limited to certain fields, but over the years, it has expanded its reach into various fields and institutions, such as architecture, art, medicine, and learning [5–7]. Photopolymerization-based 3D printing techniques have garnered significant interest among polymer chemists, material scientists, and engineers owing to noteworthy advancements in versatile polymer chemistry [8].

The approach employed in 3D photopolymerization (also known as photocuring or photocrosslinking) relies on liquid monomers and oligomers. These substances can undergo curing or photopolymerization when exposed to a light source of a specific wavelength [9]. Resins used in 3D printing are classified into several types based on their properties, chemistry, and applications [10,11]. Various resins have been used in 3D printing, including photopolymers, thermoplastics, epoxy resins, polyurethane resins, and silicone resins. Photopolymer resins are the most commonly used resins that can be cured by exposure to UV light, and are available in a range of colors, lucidities, and mechanical properties. Thermoplastic resins are suitable for rapid prototyping and small volume production. Epoxy resins provide high strength, durability, and chemical resistance for industrial tooling, molding, and casting applications. Polyurethane resins offer flexibility, toughness, impact resistance, and diverse mechanical properties for use in automotive parts, sports, and medical

Preprints (www.preprints.org) | NOT PEER-REVIEWED | Posted: 20 November 2023 doi:10.20944/preprints202311.1232.v1

devices. Silicone resins are heat- or chemically cured, providing high flexibility, heat resistance, and biocompatibility for applications, such as prosthetics, molds, and gaskets [12–16].

In addition, various photocurable additives with different chemical and mechanical properties have been used in 3D printing processes [17–19]. A photoinitiator is required to convert photolytic energy into a reactive species that can drive chain growth via radical and cationic mechanisms [20]. It is commonly used as a photoinitiator with a high molar extinction coefficient under short-wavelength UV (< 400 nm) [21–23]. Commonly used photoinitiators include camphorquinone (CQ) and diphenyl (2,4,6-trimethyl benzoyl) phosphine oxide (TPO) [24]. Reactive diluents or stabilizers can be used to control the viscosity of the resin and improve the printing characteristics of 3D printers [25,26]. The shrinkage rate during the curing process can be controlled using a reactive diluent, such as tetraethyl orthosilicate, trimethylolpropane triacrylate (TMPTMA), triethylene glycol dimethacrylate, and 3-(trimethoxysilyl)propyl methacrylate. Pigments impart color to the resin. Various colors and particle sizes are suitable for diverse applications [27–31]. A UV stabilizer protects the cured resin against discoloration and yellowing over time. Antioxidants prevent discoloration, brittleness, or cracking of the resin when exposed to oxygen or heat. Fillers, including glass fibers, carbon fibers, or metal powders, are added to increase strength, rigidity, and thermal conductivity [27,29].

The physical and mechanical properties of 3D printer resin can be reinforced using ceramic-based powders. Ceramic additives are typically used by researchers [28,32]. Zirconia is a ceramic material with high strength, toughness, and wear resistance and is the most commonly used additive [33–35]. Alumina is a ceramic material with a high strength, hardness, and chemical resistance. Silicon carbide is a ceramic with high strength, hardness, and thermal conductivity. They are widely used to improve the thermal and mechanical properties of resins. Glass was added to improve the sintering behavior and mechanical properties [36]. Glass-ceramic composites are used to improve certain properties, such as transparency and biocompatibility. Carbon is characterized by its high thermal conductivity and low density. Ceramic additives are the fastest at improving the mechanical and thermal properties of the resins [37–39].

Potassium titanate, which is synthesized by heating a mixture of potassium carbonate and titanium dioxide to high temperatures, has been studied extensively owing to its useful properties. In the early 1900s, it was utilized in electronic components owing to its excellent dielectric properties. In the mid-1900s, researchers drew attention to the field of optical properties. Research on potassium titanate expanded to new areas, including catalysis, environmental remediation, and biomedical applications, in the late 1900s. Potassium titanate can purify water and air, act as a catalyst in chemical reactions, and is biocompatible. Despite decades of research, the potential uses of potassium titanate continue to be explored, making it an attractive and promising field of study for scientists and researchers [40–42].

This study evaluated the effect of 3D printer potassium titanate/acrylate resin. SLA-printable photocurable resin formulations were prepared by mixing epoxy acrylate monomers, a difunctional urethane diacrylate crosslinker, a stabilizer consisting of an acrylate stabilizer, potassium titanate as an additive, and a photoinitiator. The mass percentage of potassium titanate affects the viscosity of the resin, print layer thickness, and mechanical properties of the fully processed product (i.e., cleaning and post-curing). Potassium titanate has a high chemical resistance and mechanical strength [43], offering the additional advantage of cost-effectiveness. The mechanical strength of the resin was measured based on its flexural strength, hardness, and tensile strength. In addition, a line pattern was designed in three dimensions using Han CAD. A line pattern model was produced using an SLA 3D printer. The leading thickness of the line pattern was designed to be a minimum of 0.2 mm and a maximum of 5.0 mm. Cracks appeared in the line pattern structure printed with a resin containing 1.5 wt% or more potassium titanate. Cracks were not observed when the stabilizer was added to the potassium titanate and acrylate resin. Furthermore, cracks did not occur even when the potassium titanate content was 1.5 wt% or higher. All potassium titanate and acrylate resins, with added stabilizers, were capable of printing line patterns up to 0.2 mm a thick. This study demonstrated the potential of potassium titanate as a new material for 3D printing. In addition, basic research on new resin materials provides data for improving resins for 3D printers and addressing their shortcomings. Therefore, material research on these new resins provides a source of technology and hidden potential for 3D printers.

2. Materials and Methods

2.1. Materials

The SLA 3D printer A+ was obtained from Shindoh Co., Ltd. (Korea), and the UV-light light-curing unit was equipped with a post-curing device (Korea).

Bisphenol-A-glycidyl dimethacrylate (Bis-EMA) were purchased from MIWON Chemical Co., Ltd., (Seoul, Korea). TMPTMA were purchased from MIWON Chemical Co. Ltd., (Korea). The urethane-acrylate copolymer used as the oligomer was obtained from Asan Materials Co., Ltd., (Korea). TPO used as a photo-initiator was purchased from MIWON Chemical Co., Ltd., (Korea). Polyethylene glycol (PEG), used as a stabilizer, was obtained from Tokyo Chemical Industry Co., Ltd., (Japan). Potassium titanate ($K_2Ti_8O_{17}$) was purchased from NewMaterials Co., Ltd., (Korea).

2.2. Methods

We prepared eleven experimental composite resins and their compositions are listed in Tables 1 and 2. All resins used in composite resins were synthesized in a ratio of bis-EMA:TMPTMA:oligomers::7.5:1:0.5 (Tables 1 and 2). The composite resin was mixed with 4 wt% TPO as a photoinitiator at 405 nm.

Table 1. Viscosity values measured for different ball-milled PEG/potassium titanate/acrylate resin dispersions.

Name	Composition (wt%)			Viscosity (cp)
	Resin	PEG	Potassium titanate	
PT0	100	0	0	975
PT05	99.5	0	0.5	1025
PT10	99	0	1.0	1231
PT15	98.5	0	1.5	1375
PT20	98	0	2.0	1452
PT30	97	0	3.0	1532
PT50	95	0	5.0	1922
PT100	90	0	10.0	3202
PT10PG10	89	10	1.0	1201
PT15PG10	88.5	10	1.5	1289
PT25PG10	87.5	10	2.5	1422

Table 2. Mechanical strength measured for different ball-milled PEG/potassium titanate/acrylate resin dispersions

Name	Flexural strength (N/mm^2)	Hardness (HV)	Tensile strength (N/mm^2)
PT0	19.45	41.5	4.95
PT05	23.74	77.7	5.93
PT10	36.63	73.9	18.2
PT15	30.12	70.0	3.03
PT20	28.45	68.2	4.51
PT30	20.11	60.0	6.56
PT50	18.94	59.5	2.86
PT100	15.21	57.9	2.32
PT10PG10	35.18	73.0	12.14

PT15PG10	38.93	79.0	15.04
PT25PG10	33.54	69.0	13.42

2.2.1. *Analysis of viscosity*

The viscosities of the resins were determined using a viscometer (DV2TLV; Rheometer, Brookfield) at a constant volume of 100 mL. The temperature of the specimens was maintained in the range of 22–25 °C. Readings were recorded at 10 rpm for 5 min in centipoise. Each specimen was measured five times, and the average value was calculated. Considering the data from the resins, viscosities of less than 2000 cp were chosen. The specimens were printed using a custom UV–SLA printer equipped with a projector (3D Printer A+, Shindoh, Korea).

2.2.2. *Analysis of flexural strength*

The flexural strength was determined using a 3-point bending test (n = 20), following the ISO 4049:2000 standard. A 3D printer was used to print rectangular specimens (1 cm× 8 cm× 0.5 cm). The printed specimens were subsequently placed in isopropyl alcohol (IPA) and washed for 10 min. Subsequently, the samples were cured for 5 min in an UV machine. Flexural strength tests were performed using a universal testing machine (UTM, Shimadzu Corporation (AGS-X)). The specimens were immersed in a 38 °C water bath for 24 h, and their thicknesses and widths were measured. The specimens were measured using the 3-point jig of a UTM (measurement conditions: speed: 1000 mm/min; load: 10 kN). The measurements were performed three times under the same conditions, and the average values were calculated.

2.2.3. *Analysis of hardness*

The hardness values of the monomer resins at different ratios were used to confirm their surface strengths. The specimens were manufactured using a polymer resin according to the specifications (2 cm × 2 cm × 2 cm; n = 5) of the 3D printer. The specimens manufactured using the 3D printer were washed and soaked in IPA to remove unreacted monomers. After removing the remaining unreacted monomer from the surface, the specimens were cured using a UV machine for approximately 5 min to polymerize the unreacted monomer and subsequently aged in an oven at 90 °C for approximately 10 h. Hardness was measured using a Durometer Digital Shore A system (Zwick Roell (Zwcik 3130, ZwickRoell GmbH&Co. KG, Ulm, Germany)). The measurement was conducted for 0–99 s with a force of 10 N using a truncated cone opening angle of 35°. The specimens were tested three times under the same conditions, and the average values were obtained.

2.2.4. *Analysis of tensile strength*

The tensile strength specimens were manufactured according to the ISO 527-2 specifications (full-length L_3 = 150 mm, parallel length L_2 = 60.0 ± 5 mm, gauge length L_1 = 108 ± 1.6 mm, thickness T = 4.0 ± 2 mm) of a 3D printer. The specimens manufactured using the 3D printer were post-processed in the same manner as in the compressed method. The tensile strength was measured using a Zwick/Roell (Z150) tester (ZwickRoell GmbH, Co. KG; Ulm, Germany). The test parameters were as follows: a load of 1 mm/min and a maximum deformation of 1%/min. The test focused on the analysis and comparison of tensile strength according to the resin.

3. Results and Discussion

Ceramic additives, including zirconia and silica, were used to improve the mechanical strength of the 3D printer resin. Potassium titanate exhibits high flexural strength, tensile strength, and toughness, while remaining compatible. This versatility opens up various potential applications. Ceramic additives affect the viscosity, precipitation, and dispersion rate of the resin depending on their content. A high additive content improved the mechanical strength and thermal properties of the resin. Photocurable resins were prepared by mixing epoxy acrylate monomers with a difunctional urethane diacrylate crosslinker (Figure 1a). Potassium titanate was added to the 0–10 wt% to the

 doi:10.20944/preprints202311.1232.v1

resin. Additionally, PEG was used as a stabilizer to adjust the viscosity of the potassium titanate/acrylate resin. The amount of stabilizer used was 10 wt% of the total resin mass. Excessive amounts of the stabilizers affect the physical and mechanical properties of resin [44]. Figure 1b shows the SEM images of the powder surface used for the 3D printer resin. Potassium titanate powder was prepared by ball milling at 120 rpm for 24 h. In addition, the powder was separated using a 200 μm sieve. Figure 1c shows the schematic of the SLA printer. The resolution of the acrylate resin used for SLA can vary depending on the depth of light penetration. In general, ceramic resins employed in SLA printers should ideally have low viscosity, typically below 3000 cp, to facilitate self-leveling during the 3D printing process. This remains true even when the viscosity of these resins increases exponentially with increasing ceramic content [45,46]. Figure 1e shows SEM images representing the mechanical strength of the specimen surface. Figure 1f shows the printed curved pattern structure. Figure 1g shows a printed hemisphere structure such as an isotropic truss structure. The potassium titanate/acrylate resin demonstrated 3D printing capabilities by fabricating complex geometric structures (Figures 1f and g). Potassium titanate/acrylate resin produces 3D printed structures with smooth surfaces, thus providing high printing resolution and accuracy. Additionally, potassium titanate/acrylate resin successfully produced structures without any defects or delamination, which is critical for 3D printer applications.

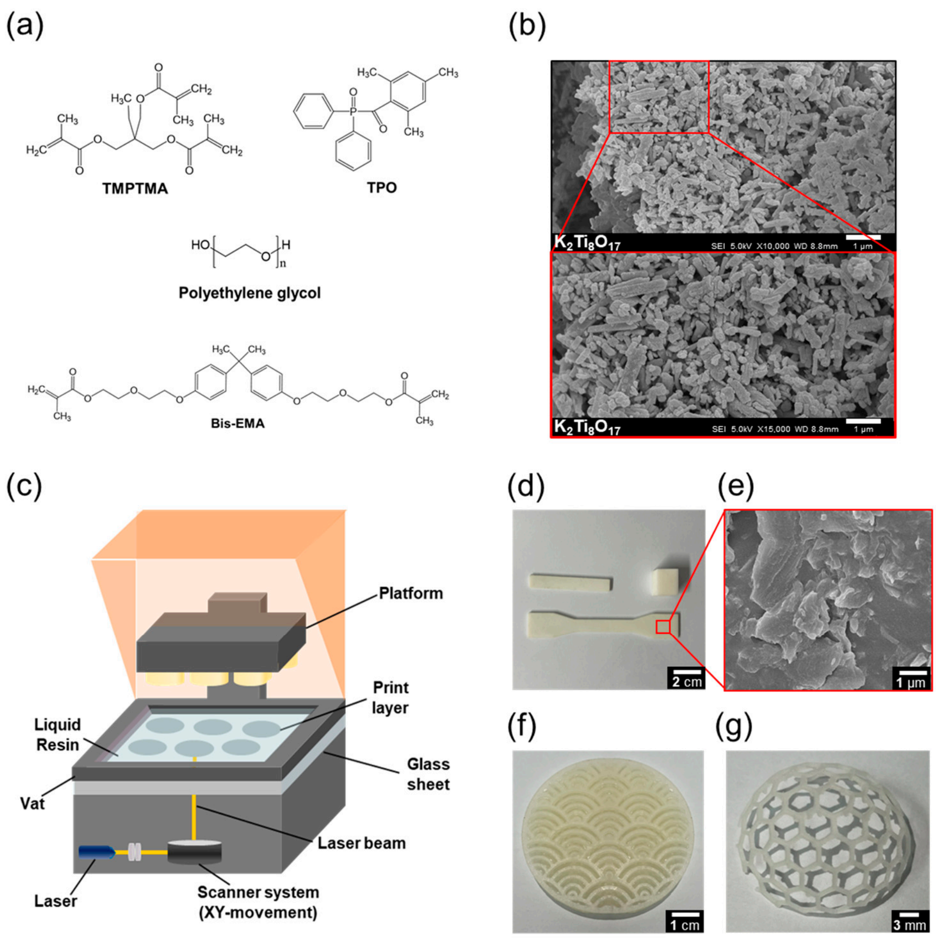

Figure 1. (A) The chemical structures of the monomers (Bis-GMA, triethylene glycol dimethacrylate, and polyethylene glycol (PEG)) and initiator diphenyl (2,4,6-trimethyl benzoyl) phosphine oxide used in the synthesis of the 3D photopolymerization resin, (B) SEM image of potassium titanate powder (10,000× magnification, 15,000× magnification), (C) Image of SLA setup, (D) Printed specimens sample for mechanical strength measurement, (E) and SEM magnified image of mechanical strength surface, (F) Image of the curved pattern structure with a 3D printer , (G) Image of the three-dimensional fullerene structure with a 3D printer.

Preprints (www.preprints.org) | NOT PEER-REVIEWED | Posted: 20 November 2023 doi:10.20944/preprints202311.1232.v1

The number of acrylate groups in UV-curable monomers generally affects the crosslinking reaction and the mechanical properties of the cured body. In the experiments, missing layers appeared in the resin printouts when the viscosity of the potassium titanate/acrylate resin exceeded 2000 cp. In this study, a photoinitiator with an absorption peak in the range of 350–420 nm was used for the photopolymerization reaction. Typically, the initiators used for the photopolymerization of resins are CQ and TPO. CQ has a visible-light absorption peak in the range of 380–520 nm. TPO has an absorption peak in the range 380–425 nm. We used TPO for the potassium titanate/acrylate resin (Figure 1a) because the polymerization efficiency of TPO is higher than that of CQ. In addition, the TPO initiator changes from pale yellow to transparent upon exposure to UV light.

3.1. Viscosity of potassium titanate/acrylate resin using ceramic-based additive

The polymerization rate of the resin affects the mobility of monomers and free radicals. Therefore, it is correlated with the initial viscosity of the resin. The viscosity of potassium titanate/acrylate resin tends to increase with the amount of potassium titanate (Table 1) [8,11]. For resins PT0–PT100, the weight ratio of potassium titanate was increased to 0–10 wt%. As shown in Figure 2a, the viscosity increases to 975–3202 as the amount of potassium titanate increases. The difference in viscosity between PT0 and PT100 was approximately 3.2 times. In addition, cracks and undispersed potassium titanate powder were observed in the structure printed with a resin of 3000 cp or higher. Therefore, a small amount of PEG was added to adjust viscosity and dispersion (Table 1). The viscosity of the resin decreased by 1.5–3% after addition of PEG (Figure 2b).

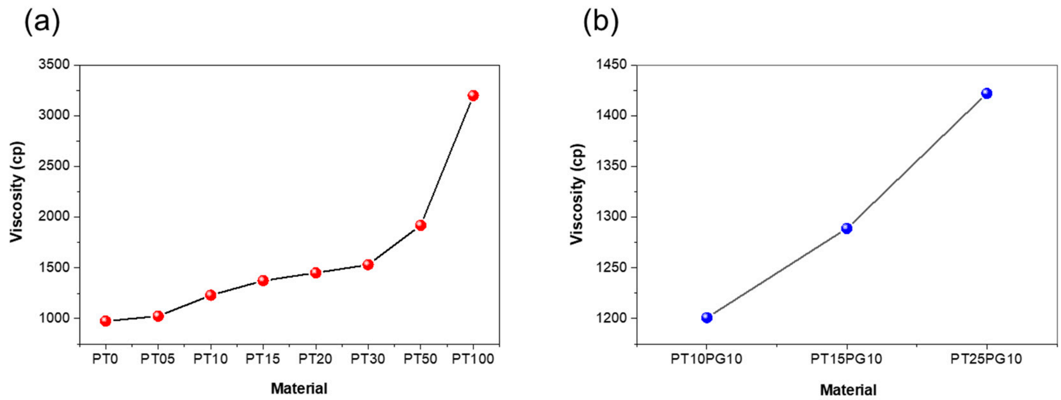

Figure 2. Viscosity of 3D printer resin. (a) Potassium titanate/acrylate resin, (b) PEG/potassium titanate/acrylate resin.

3.2. Mechanical properties of potassium titanate/acrylate resin using ceramic-based additive

The amount of ceramic additive in the resin significantly affected the mechanical strength. Potassium titanate particles distribute the stress throughout the resin and prevent cracking. The addition of the potassium titanate powder increased the surface area of the material. In addition, the potassium titanate powder provided more contact points between the powder particles and the resin matrix. The enlarged contact area enhanced the bonding between the two materials, resulting in a stronger composite material and improved strength [31,32,35].

As summarized in Table 2, the mechanical properties of the potassium titanate/acrylate resin first increased and then decreased as the potassium titanate powder content increased. In addition, as the PEG content increased from 0 to 10 wt%, the flexural strength, tensile strength, and hardness of the potassium titanate/acrylate resin gradually increased. The flexural strength values are shown in Figure 3. PT10 exhibited the highest flexural strength of 36 ± 2 N/mm^2. PT100 exhibited the lowest flexural strength of 15 ± 3 N/mm^2. PT100 was lower than that of PT0 without potassium titanate. Figure 3a shows that the flexural strength was highest when the potassium titanate content was 1 wt%. In addition, when the potassium titanate content was 1 wt% or higher, the flexural strength

 doi:10.20944/preprints202311.1232.v1

decreased. However, when comparing PT15 and PT15PG10, PT15PG10 with PEG exhibited higher flexural strength (Figure 3b). PT15PG10 exhibited the highest flexural strength of 39 ± 1 N/mm².

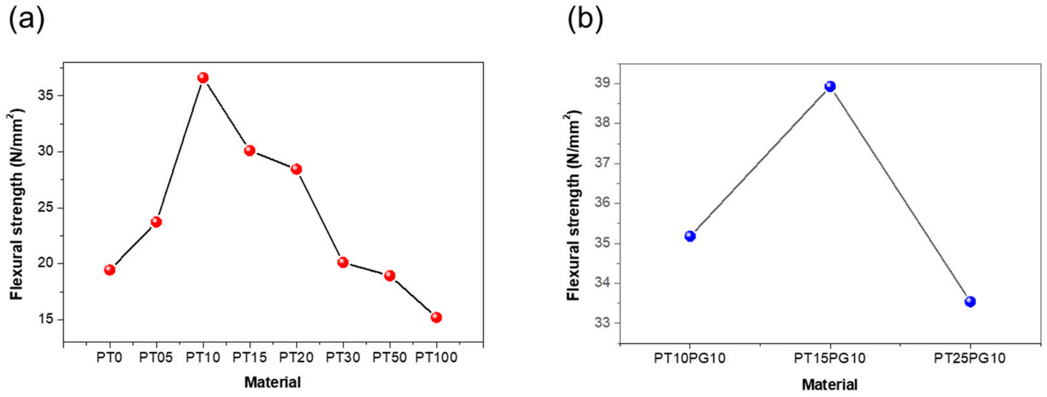

Figure 3. Flexural strength of 3D printed specimens. (a) Potassium titanate/acrylate resin, (b) PEG/potassium titanate/acrylate resin.

Figure 4 shows the surface hardness values. The 3D-printed cube with PT15PG10 exhibited the highest surface hardness of 79.0 ± 1.2 HV. PT0 showed the lowest surface hardness values of 41.5 ± 0.5 MV. The surface hardness of the resin containing a high amount of potassium titanate was lower than that of the resin containing 10 wt% PEG. Even with the same amount of potassium titanate, the amount of resin with PEG was higher (Figure 4b). The PT15 and PT15PG10 values were 70.0 ± 2.0 HV and 79.0 ± 1.2 HV. The difference between the two values was approximately 11%. PT15PG10, with PEG, exhibited the highest values. The stabilizer helped evenly disperse the potassium titanate powder in the resin. Potassium titanate is distributed throughout the resin and increases its strength by reducing the stress concentrations and preventing cracking.

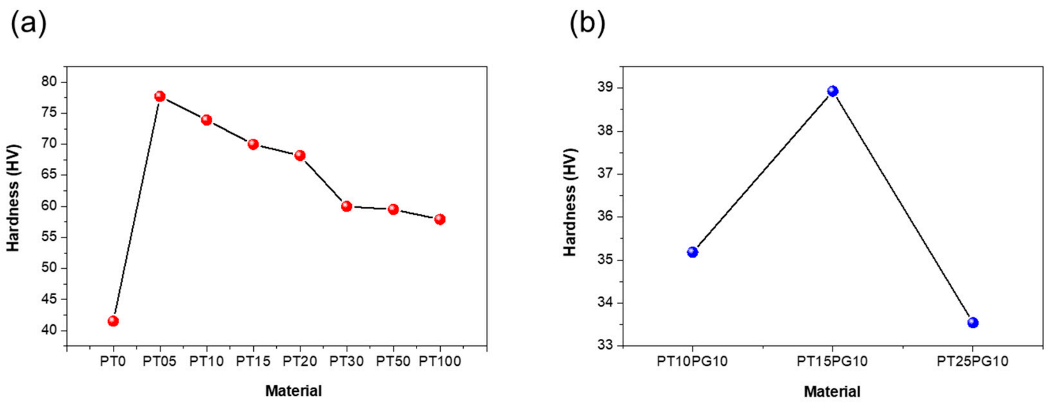

Figure 4. Surface hardness of 3D printed specimens. (a) Potassium titanate/acrylate resin, (b) PEG/potassium titanate/acrylate resin.

Figure 5 shows a trend similar to the measurement results for the flexural strength and hardness. The PT10 specimen exhibited the highest tensile strength at 18.0 N/mm². However, the potassium titanate content rapidly decreased from 1 wt% or higher. PT100 exhibits the lowest tensile strength of 2.32 N/mm² (Figure 5). The difference from the sample without PEG was greater than 10 N/mm², except for that of the PT10 specimen.

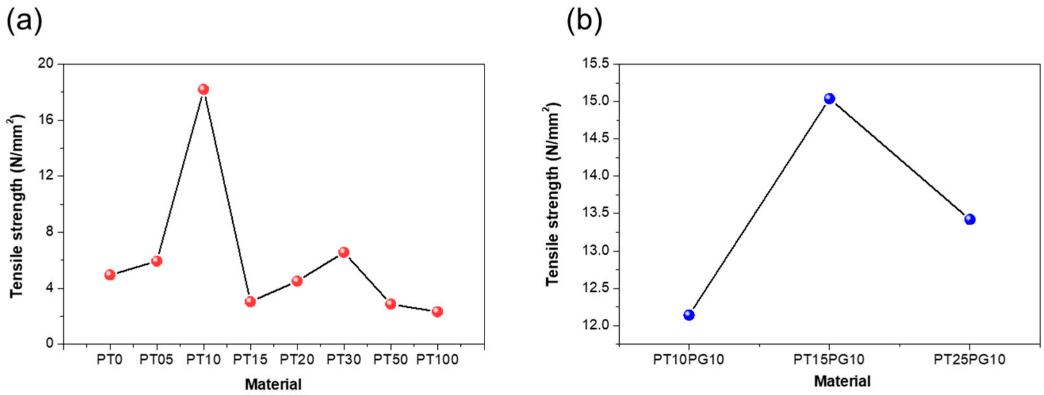

Figure 5. Tensile strength of 3D printed specimens. (a) Potassium titanate/acrylate resin, (b) PEG/potassium titanate/acrylate resin.

The mechanical strength results indicated that the resin containing PEG exhibited a higher mechanical strength. Although potassium titanate improved the mechanical strength of the resin, the mechanical strength decreased when a certain limit was exceeded. In this case, the potassium titanate content can be increased using a stabilizer. The flexural strength of PT15 was 30.12 N/mm^2. However, the flexural strength of PT15PG10 with a small amount of stabilizer was 38.93 N/mm^2. The hardness of PT15 was 70.0 N/mm^2. The hardness of PT15PG10 was 79.0 N/mm^2. Therefore, a small amount of stabilizer increased the dispersion rate of potassium titanate, further increasing the strength of the resin [39].

3.3. 3D Printing of potassium titanate/acrylate resin using ceramic-based additive

The color and transparency of the photocurable resin affect the output of the structure. The amount of light absorbed varied according to the transparency of the resin. The absorption of insufficient light can lead to structural cracks. Additionally, excess additives precipitate at the bottom of the resin bath and obstruct the light irradiation. Therefore, it is necessary to verify the resolution of the resin based on its additive content. Line patterns were designed using HAN CAD. The line pattern support was prepared (width = 3.2 cm; length = 6 cm; height = 3 mm). The line thickness range of the entire line pattern was 0.2 to 5 mm. The line pattern thickness was divided into the ranges of 0.2 to 1 mm and 1 to 5 mm. We designed a 9-line thickness pattern up to 0.2 to 1 mm in 0.1 mm increments (Figure 6). We designed a 5-line thickness pattern of 1–5 mm in 1 mm increments. As shown in Figure 6, the resin with a low amount of potassium titanate exhibited better line pattern resolution. In addition, the resin of the PT10PG10-containing stabilizer showed a resolution of up to 0.2 mm. Consequently, a resin printed with a very thin and detailed printing pattern shows good resolution as a resin for 3D printers.

Preprints (www.preprints.org) | NOT PEER-REVIEWED | Posted: 20 November 2023 doi:10.20944/preprints202311.1232.v1

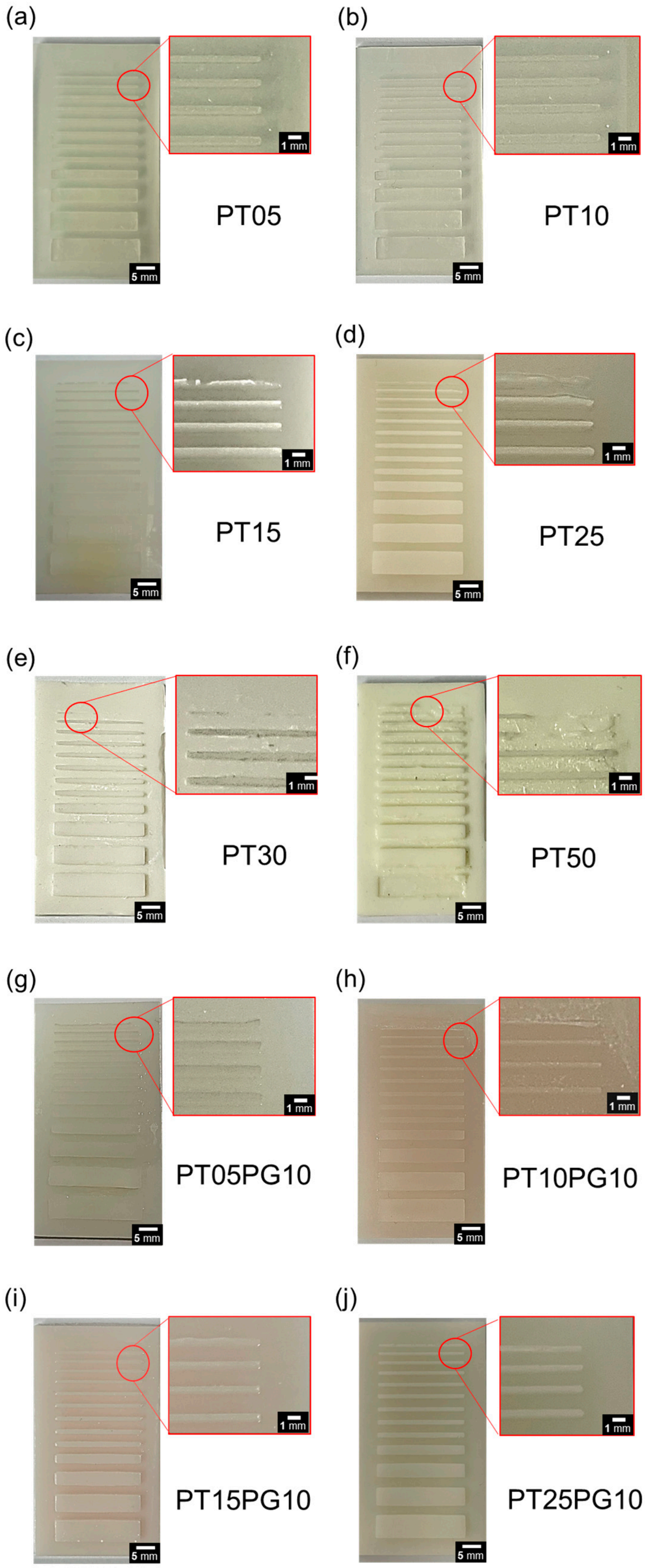

Figure 6. 3D printed line pattern using potassium titianate resins (The line thickness range from 0.2 to 5 mm) as a photoinitiating system for the polymerization of the 3D resin, (a) line pattern image printed with resin containing 0.5 wt% of potassium titanate, (b) resin containing 1.0 wt% of potassium titanate, (c) resin containing 1.5 wt% of potassium titanate, (d) resin containing 2.5 wt% of potassium titanate, (e) resin containing 3.0 wt% of potassium titanate, (f) resin containing 5.0 wt% of potassium

titanate, (g) line pattern image printed with resin containing 0.5 wt% of potassium titanate and 10 wt% PEG, (h) resin containing 1.0 wt% of potassium titanate and 10 wt% PEG, (i) resin containing 1.5 wt% of potassium titanate and 10 wt% PEG, (j) resin containing 2.5 wt% of potassium titanate and 10 wt% PEG.

The resins used in 3D printing have a wide range of applications and must be optimized for each condition and environment. The field of crafts requires detailed and sophisticated work. Therefore, the main advantages of resin are its high resolution and saturation. In medical applications, these two conditions are distinct. This result depend on whether the printed structure is placed inside or outside the human body. Toxicity and biocompatibility testing are also critical when 3D-printed structures are used in medical applications. Industrial applications require excellent mechanical properties to withstand pressure and impact [47,48].

Therefore, it is necessary to test the mechanical properties of the resin after the addition of pigments [37,49]. Furthermore, the resolution and stability of a pigmented resin may vary over time owing to precipitation. Therefore, the precipitation of the resin and manufacturing period must be considered when performing stability and resolution tests. Toxicity and biocompatibility tests should be conducted with and without pigment addition, and by varying the monomer resin ratio [48,50,51].

4. Conclusions

This study utilized potassium titanate powder as an additive to enhance the mechanical strength of acrylate resin. The mechanical strength and resolution of the resin were compared before and after using the stabilizer. The stabilizer enhanced the bonding force with the resin matrix, resulting in an increase in the mechanical strength of the resin. The line pattern thickness of 0.2 mm was successfully printed using PEG, potassium titanate, and acrylate resin. This study provides the possibility that potassium titanate can be used in diverse 3D printing industries for the first time by applying potassium titanate to 3D printers. Research on such materials is necessary to develop a 3D printer market and technology. Prior to the commercialization of potassium titanate and acrylate resins, additional studies on the precipitation of potassium titanate, resin stability, biocompatibility, and toxicity should be conducted.

Author Contributions: Conceptualization, N.C., S.J. and Y.C.; methodology, N.C. and Y.C.; software, Y.C., J.K.; validation, N.C., C.L. and Y.C.; formal analysis, G.L., Y.C.; investigation, Y.C.; resources, N.C. and S.J.; data curation, N.C., Y.C.; writing—original draft preparation, N.C., Y.C.; writing—review and editing, N.C. and Y.C.; visualization, Y.C.; supervision, N.C. and S.J.; project administration, N.C. and S.J.; funding acquisition, N.C., S.J. and Y.C. All authors have read and agreed to the published version of the manuscript.

Funding: This study was supported by the Soonchunhyang University Research Fund(grant number 20210132).

Institutional Review Board Statement: Not applicable.

Data Availability Statement: Not applicable.

Conflicts of Interest: The authors declare no conflict of interest.

References

1. Ligon, S.C.; Liska, R.; Stampfl, J.; Gurr, M.; Mülhaupt, R. Polymers for 3D Printing and Customized Additive Manufacturing. *Chemical Reviews* **2017**, *117*, 10212-10290, doi:10.1021/acs.chemrev.7b00074.
2. Jain, A.; Bansal, K.K.; Tiwari, A.; Rosling, A.; Rosenholm, J.M. Role of Polymers in 3D Printing Technology for Drug Delivery - An Overview. *Curr Pharm Des* **2018**, *24*, 4979-4990, doi:10.2174/1381612825666181226160040.
3. Jungst, T.; Smolan, W.; Schacht, K.; Scheibel, T.; Groll, J. Strategies and Molecular Design Criteria for 3D Printable Hydrogels. *Chemical Reviews* **2016**, *116*, 1496-1539, doi:10.1021/acs.chemrev.5b00303.
4. Wendel, B.; Rietzel, D.; Kühnlein, F.; Feulner, R.; Hülder, G.; Schmachtenberg, E. Additive Processing of Polymers. *Macromolecular Materials and Engineering* **2008**, *293*, 799-809, doi:10.1002/mame.200800121.
5. Berman, B. 3-D printing: The new industrial revolution. *Business Horizons* **2012**, *55*, 155-162, doi:https://doi.org/10.1016/j.bushor.2011.11.003.

6. Kwon, I.K.; Matsuda, T. Photo-polymerized microarchitectural constructs prepared by microstereolithography (muSL) using liquid acrylate-end-capped trimethylene carbonate-based prepolymers. *Biomaterials* **2005**, *26*, 1675-1684, doi:10.1016/j.biomaterials.2004.06.041.
7. Melchels, F.P.; Feijen, J.; Grijpma, D.W. A review on stereolithography and its applications in biomedical engineering. *Biomaterials* **2010**, *31*, 6121-6130, doi:10.1016/j.biomaterials.2010.04.050.
8. Layani, M.; Wang, X.; Magdassi, S. Novel Materials for 3D Printing by Photopolymerization. *Advanced Materials* **2018**, *30*, 1706344, doi:10.1002/adma.201706344.
9. Fu, J.; Yin, H.; Yu, X.; Xie, C.; Jiang, H.; Jin, Y.; Sheng, F. Combination of 3D printing technologies and compressed tablets for preparation of riboflavin floating tablet-in-device (TiD) systems.
10. Harynska, A.; Kucinska-Lipka, J.; Sulowska, A.; Gubanska, I.; Kostrzewa, M.; Janik, H. Medical-Grade PCL Based Polyurethane System for FDM 3D Printing-Characterization and Fabrication. *Materials (Basel)* **2019**, *12*, 887, doi:10.3390/ma12060887.
11. Ivanova, O.; Williams, C.; Campbell, T. Additive manufacturing (AM) and nanotechnology: promises and challenges. *Rapid Prototyping Journal* **2013**, *19*, 353-364, doi:10.1108/Rpj-12-2011-0127.
12. Ullett, J.S.; Schultz, J.W.; Chartoff, R.P. Novel liquid crystal resins for stereolithography - processing parameters and mechanical analysis. *Rapid Prototyping Journal* **2000**, *6*, 8-17, doi:Doi 10.1108/13552540010309840.
13. Vaezi, M.R.; Seitz, H.; Yang, S. A review on 3D micro-additive manufacturing technologies. *The International Journal of Advanced Manufacturing Technology* **2013**, *67*, 1721-1754, doi:10.1007/s00170-012-4605-2.
14. Revilla-León, M.; Özcan, M. Additive Manufacturing Technologies Used for Processing Polymers: Current Status and Potential Application in Prosthetic Dentistry: Polymer Additive Manufacturing for Prosthodontics. *Journal of Prosthodontics* **2018**, *28*, 146-158, doi:10.1111/jopr.12801.
15. Hector Sandoval, J.; Wicker, R.B. Functionalizing stereolithography resins: effects of dispersed multi-walled carbon nanotubes on physical properties. *Rapid Prototyping Journal* **2006**, *12*, 292-303, doi:10.1108/13552540610707059.
16. Dizon, J.R.C.; Espera, A.H.; Chen, Q.; Advincula, R.C. Mechanical characterization of 3D-printed polymers. *Additive Manufacturing* **2018**, *20*, 44-67, doi:https://doi.org/10.1016/j.addma.2017.12.002.
17. Shukla, V.; Bajpai, M.; Singh, D.K.; Singh, M.; Shukla, R. Review of basic chemistry of UV-curing technology. *Pigment & Resin Technology* **2004**, *33*, 272-279, doi:10.1108/03699420410560461.
18. Cornelio, R.B.; Wikant, A.; Mjosund, H.; Kopperud, H.M.; Haasum, J.; Gedde, U.W.; Ortengren, U.T. The influence of bis-EMA vs bis GMA on the degree of conversion and water susceptibility of experimental composite materials. *Acta Odontol Scand* **2014**, *72*, 440-447, doi:10.3109/00016357.2013.856467.
19. Travitzky, N.; Bonet, A.; Dermeik, B.; Fey, T.; Filbert-Demut, I.; Schlier, L.; Schlordt, T.; Greil, P. Additive Manufacturing of Ceramic-Based Materials. *Advanced Engineering Materials* **2014**, *16*, 729-754, doi:10.1002/adem.201400097.
20. Mondschein, R.J.; Kanitkar, A.; Williams, C.B.; Verbridge, S.S.; Long, T.E. Polymer structure-property requirements for stereolithographic 3D printing of soft tissue engineering scaffolds.
21. Kim, G.-T.; Go, H.-B.; Yu, J.-H.; Yang, S.-Y.; Kim, K.-M.; Choi, S.-H.; Kwon, J.-S. Cytotoxicity, Colour Stability and Dimensional Accuracy of 3D Printing Resin with Three Different Photoinitiators. *Polymers* **2022**, *14*, 979.
22. Zhang, J.; Launay, K.; Hill, N.S.; Zhu, D.; Cox, N.; Langley, J.; Lalevée, J.; Stenzel, M.H.; Coote, M.L.; Xiao, P. Disubstituted Aminoanthraquinone-Based Photoinitiators for Free Radical Polymerization and Fast 3D Printing under Visible Light. *Macromolecules* **2018**, *51*, 10104-10112, doi:10.1021/acs.macromol.8b02145.
23. Dadashi-Silab, S.; Aydogan, C.; Yagci, Y. Shining a light on an adaptable photoinitiator: advances in photopolymerizations initiated by thioxanthones. *Polymer Chemistry* **2015**, *6*, 6595-6615, doi:10.1039/C5PY01004G.
24. Meereis, C.T.; Leal, F.B.; Lima, G.S.; de Carvalho, R.V.; Piva, E.; Ogliari, F.A. BAPO as an alternative photoinitiator for the radical polymerization of dental resins.
25. Zhang, K.; Xie, C.; Wang, G.; He, R.; Ding, G.; Wang, M.; Dai, D.; Fang, D. High solid loading, low viscosity photosensitive Al2O3 slurry for stereolithography based additive manufacturing. *Ceramics International* **2019**, *45*, 203-208, doi:https://doi.org/10.1016/j.ceramint.2018.09.152.
26. Ding, G.; He, R.; Zhang, K.; Xia, M.; Feng, C.; Fang, D. Dispersion and stability of SiC ceramic slurry for stereolithography. *Ceramics International* **2020**, *46*, 4720-4729, doi:https://doi.org/10.1016/j.ceramint.2019.10.203.
27. Lemon, M.T.; Jones, M.S.; Stansbury, J.W. Hydrogen bonding interactions in methacrylate monomers and polymers. *J Biomed Mater Res A* **2007**, *83*, 734-746, doi:10.1002/jbm.a.31448.
28. Crivello, J.V.; Reichmanis, E. Photopolymer Materials and Processes for Advanced Technologies. *Chemistry of Materials* **2014**, *26*, 533-548, doi:10.1021/cm402262g.

29. Ferracane, J.L. Resin composite--state of the art. *Dent Mater* **2011**, *27*, 29-38, doi:10.1016/j.dental.2010.10.020.
30. Song, Y.; Zheng, Y.L.; Tang, Y.F.; Yang, H.B. Fabrication and Stability of CoAl2O4 Ceramic Pigment for 3D Printing. *Materials Science Forum* **2017**, *898*, 1935-1939, doi:10.4028/www.scientific.net/MSF.898.1935.
31. Chung, K.; Greener, E.H. Degree of conversion of seven visible light-cured posterior composites. *J Oral Rehabil* **1988**, *15*, 555-560, doi:10.1111/j.1365-2842.1988.tb00192.x.
32. dos Santos, G.B.; Alto, R.V.; Filho, H.R.; da Silva, E.M.; Fellows, C.E. Light transmission on dental resin composites. *Dent Mater* **2008**, *24*, 571-576, doi:10.1016/j.dental.2007.06.015.
33. Zhang, X.; Wu, X.; Shi, J. Additive manufacturing of zirconia ceramics: a state-of-the-art review. *Journal of Materials Research and Technology* **2020**, *9*, 9029-9048, doi:https://doi.org/10.1016/j.jmrt.2020.05.131.
34. Qin, W.; Majidi, H.; Yun, J.; van Benthem, K. Electrode Effects on Microstructure Formation During FLASH Sintering of Yttrium-Stabilized Zirconia. *Journal of the American Ceramic Society* **2016**, *99*, 2253-2259, doi:https://doi.org/10.1111/jace.14234.
35. Manicone, P.F.; Rossi Iommetti, P.; Raffaelli, L. An overview of zirconia ceramics: Basic properties and clinical applications. *Journal of Dentistry* **2007**, *35*, 819-826, doi:https://doi.org/10.1016/j.jdent.2007.07.008.
36. Suominen, J.M.; Frankberg, E.J.; Vallittu, P.K.; Levänen, E.; Vihinen, J.; Vastamäki, T.; Kari, R.; Lassila, L.V.J. Three-dimensional printing of zirconia: characterization of early stage material properties. *Biomaterial Investigations in Dentistry* **2019**, *6*, 23-31, doi:10.1080/26415275.2019.1640608.
37. Wesemann, C.; Spies, B.C.; Sterzenbach, G.; Beuer, F.; Kohal, R.; Wemken, G.; Krügel, M.; Pieralli, S. Polymers for conventional, subtractive, and additive manufacturing of occlusal devices differ in hardness and flexural properties but not in wear resistance. *Dent Mater* **2021**, *37*, 432-442, doi:10.1016/j.dental.2020.11.020.
38. Piconi, C.; Maccauro, G. Zirconia as a ceramic biomaterial. *Biomaterials* **1999**, *20*, 1-25, doi:https://doi.org/10.1016/S0142-9612(98)00010-6.
39. Alarifi, I.M. A performance evaluation study of 3d printed nylon/glass fiber and nylon/carbon fiber composite materials. *Journal of Materials Research and Technology* **2022**, *21*, 884-892, doi:https://doi.org/10.1016/j.jmrt.2022.09.085.
40. Marchand, R.; Brohan, L.; Tournoux, M. TiO2(B) a new form of titanium dioxide and the potassium octatitanate K2Ti8O17. *Materials Research Bulletin* **1980**, *15*, 1129-1133, doi:https://doi.org/10.1016/0025-5408(80)90076-8.
41. Suganuma, K.; Fujita, T.; Niihara, K.; Suzuki, N. AA6061 composite reinforced with potassium titanate whisker. *Journal of Materials Science Letters* **1989**, *8*, 808-810, doi:10.1007/BF01730145.
42. Minjie Qu, X.J.W.H.E.G.L. Performance of Potassium Titanate Whisker Reinforced PPESK Composites. *Journal of Materials Sciences and Technology* **2009**, *20*, 445-447.
43. Jiang, W.; Tjong, S.C. Thermal stability of polycarbonate composites reinforced with potassium titanate whiskers: effect of coupling agent addition. *Polymer Degradation and Stability* **1999**, *66*, 241-246, doi:https://doi.org/10.1016/S0141-3910(99)00072-5.
44. Song, S.Y.; Park, M.S.; Lee, D.; Lee, J.W.; Yun, J.S. Optimization and characterization of high-viscosity ZrO2 ceramic nanocomposite resins for supportless stereolithography. *Materials & Design* **2019**, *180*, 107960, doi:https://doi.org/10.1016/j.matdes.2019.107960.
45. Faes, M.; Vleugels, J.; Vogeler, F.; Ferraris, E. Extrusion-based additive manufacturing of ZrO2 using photoinitiated polymerization. *CIRP Journal of Manufacturing Science and Technology* **2016**, *14*, 28-34, doi:https://doi.org/10.1016/j.cirpj.2016.05.002.
46. Lian, Q.; Sui, W.; Wu, X.; Yang, F.; Yang, S. Additive manufacturing of ZrO ceramic dental bridges by stereolithography. *Rapid Prototyping Journal* **2018**, *24*, 114-119, doi:10.1108/RPJ-09-2016-0144.
47. Jl, F.; EH, G. Fourier transform infrared analysis of degree of polymerization in unfilled resins--methods comparison. *J Dent Res* **1984**, *63*, 1093-1095, doi:10.1177/00220345840630081901.
48. Pelka, M.; Danzl, C.; Distler, W.; Petschelt, A. A new screening test for toxicity testing of dental materials. *Journal of Dentistry* **2000**, *28*, 341-345, doi:https://doi.org/10.1016/S0300-5712(00)00007-5.
49. Goncalves, F.; Campos, L.M.P.; Rodrigues-Junior, E.C.; Costa, F.V.; Marques, P.A.; Francci, C.E.; Braga, R.R.; Boaro, L.C.C. A comparative study of bulk-fill composites: degree of conversion, post-gel shrinkage and cytotoxicity. *Braz Oral Res* **2018**, *32*, e17, doi:10.1590/1807-3107bor-2018.vol32.0017.
50. Warr, C.; Valdoz, J.C.; Bickham, B.P.; Knight, C.J.; Franks, N.A.; Chartrand, N.; Van Ry, P.M.; Christensen, K.A.; Nordin, G.P.; Cook, A.D. Biocompatible PEGDA Resin for 3D Printing. *ACS Applied Bio Materials* **2020**, *3*, 2239-2244, doi:10.1021/acsabm.0c00055.
51. Lin, C.-H.; Lin, Y.-M.; Lai, Y.-L.; Lee, S.-Y. Mechanical properties, accuracy, and cytotoxicity of UV-polymerized 3D printing resins composed of Bis-EMA, UDMA, and TEGDMA. *The Journal of Prosthetic Dentistry* **2020**, *123*, 349-354, doi:https://doi.org/10.1016/j.prosdent.2019.05.002.

 doi:10.20944/preprints202311.1232.v1